Long Island Sound Coastal Observatory: assessment of above-water radiometric measurement uncertainties using collocated multi and hyper-spectral systems: reply to comment

Tristan Harmel,[1,*] Alexander Gilerson,[2] Soe Hlaing,[2] Alan Weidemann,[3] Robert Arnone,[3] and Samir Ahmed[2]

[1]Laboratoire d'Océanographie de Villefranche, Université Pierre et Marie Curie, Centre National de la Recherche Scientifique, Villefranche-sur-Mer, France

[2]Optical Remote Sensing Laboratory, The City College of the City University of New York, New York 10031, USA

[3]Naval Research Laboratory, Stennis Space Center, Mississippi 39529, USA

*Corresponding author: harmel@obs-vlfr.fr

Received 6 March 2012; revised 2 April 2012; accepted 11 April 2012; posted 13 April 2012 (Doc. ID 164189); published 8 June 2012

Uncertainties associated with the derivation of the exact normalized water-leaving radiance (L_{WN}) from an above-water radiometric system were analyzed in Harmel *et al.* [Appl. Opt. **50**, 5842 (2011)] based on collocated hyperspectral (HyperSAS) and multispectral (SeaPRISM) systems installed on the Long Island Sound Coastal Observational (LISCO) platform. Based on a 1.5 year time series of LISCO data, uncertainty contributors in the derivation of $\boldsymbol{L_{WN}}$ were quantified in units of unbiased relative percentage differences (URPD) by applying the different steps of the respective data processing incrementally. Results showed that discrepancy between $\boldsymbol{L_{WN}}$ data of two systems is significantly reduced when the average total sea radiance data of SeaPRISM is used in lieu of the standard one, which utilizes only the lowest total sea radiance measurements to remove the sky glint perturbations. The Zibordi comment [Appl. Opt. **51**, 3888 (2012)] rejects the conclusion that attributes the sky glint removal step as the major uncertainty contributor in the SeaPRISM processing. It then states that the observed discrepancy might be due to an increased probability of sun-glint contamination in HyperSAS measurements because of its wider field of view and longer integration time. It was also underlined that observed dispersion between the atmospheric transmittance data derived from HyperSAS and SeaPRISM measurements can be attributed to probable contamination by stray light perturbation or issues with the noncosine response of the HyperSAS irradiance sensor. Finally, it was suggested to thoroughly investigate those instrumental perturbations. In this reply, impacts of nonperfect cosine response of the irradiance sensor are shown to be relatively low (<2% on average) and therefore can only partially explain the bias in atmospheric transmittance. Additional discrepancies between the HyperSAS and SeaPRISM downwelling irradiance derivation are attributed to the presence of absorbing aerosols. Intercomparisons of the total sea radiance and nonnormalized water-leaving radiance, complementary to those discussed in the LISCO paper, are analyzed, and this analysis shows that discrepancies in normalized water-leaving radiance retrievals arise from data processing and not from instrumental uncertainty. In addition, limitations in the standard data processing to meaningfully derive normalized water-leaving radiance for various appropriate viewing configurations are discussed. It is finally advocated that the issue of sky glint perturbation correction requires further analysis based on radiative transfer computations, including refined modeling of wave slope distributions.

OCIS codes: 010.0010, 280.0280, 010.4450, 010.1320, 110.4234.

1559-128X/12/173893-07$15.00/0

1. Introduction

Above-water radiometric instrumentation, such as that developed within the framework of the Ocean Color component of the Aerosol Robotic Network (AERONET-OC), offers reliable performance over long periods of time to monitor the water-leaving radiance [1]. This radiometric product is operationally utilized for water-quality monitoring and the validation of ocean color satellite products [2,3]. However, one of the major difficulties of above-water measurements is to correct observations for the impact of sunlight (sun glint) and skylight (sky glint) components, which are reflected by the ruffled sea surface [4]. Thus, sophisticated data processing is needed to retrieve the water-leaving radiance from the raw measurements.

In the paper on "Long Island Sound Coastal Observatory (LISCO)" by Harmel *et al.* [5], the setup and the data processing of two collocated above-water radiometric systems have been described. These are the Hyperspectral Surface Acquisition System (HyperSAS, Satlantic Inc., Canada) and the Sea-Viewing Wide Field-of-View Sensor (SeaWiFS) Photometer Revision for Incident Surface Measurements (SeaPRISM, CE-318, CIMEL France), which is part of the AERONET-OC network. In this study, the uncertainty analysis of the LISCO data was based on intercomparison of HyperSAS and SeaPRISM data over a 1.5 year period for each intermediate step of the data processing applied incrementally. It should be noted that intercomparisons were obtained with different azimuth angles of SeaPRISM and HyperSAS, which includes very different sky radiances and more challenging correction for the bidirectional effect in coastal waters.

In the comment paper by Zibordi [6], it is advanced that the standard data processing might create an overcorrection of sky-glint perturbations but certainly not one that entirely explains the observed differences between HyperSAS and SeaPRISM unbiased absolute differences. It is also argued that the discrepancies observed in the LISCO data sets might originate from the instrument performance (e.g., polarization sensitivity and stray light perturbations relevant for hyperspectral systems, noncosine response relevant for irradiance sensors), uncertainties in absolute calibration, environmental perturbations, and finally uncertainties related to input parameters applied for data processing. In this reply, the noncosine response of the HyperSAS irradiance sensor is first addressed. Next, the intercomparisons of the HyperSAS and SeaPRISM datasets are completed with a complementary analysis of the total and nonnormalized water-leaving radiances to further evaluate the impact of the correction for the sea surface reflected light on the uncertainty budget. Finally, a commentary addressing ways of further improving this correction step is provided in the last section.

2. Intercomparison Results from LISCO Site

A. Statistical Estimators

The same data sets as those used in the LISCO paper are used to conduct intercomparison between HyperSAS and SeaPRISM products. To discuss the intercomparison, statistical quantities similar to those of the Zibordi comment have been used to allow for a direct comparison between the two studies. The average of unbiased relative percent difference (URPD) and the average of its absolute value (|URPD|) are defined as follows:

$$\mathrm{URPD} = 200 \times \frac{1}{N}\sum_{i=1}^{N}\frac{y_i - x_i}{x_i + y_i}, \tag{1}$$

$$|\mathrm{URPD}| = 200 \times \frac{1}{N}\sum_{i=1}^{N}\left|\frac{y_i - x_i}{x_i + y_i}\right|, \tag{2}$$

where x stands for SeaPRISM data and y for HyperSAS data, N being the number of matchup points available. The root-mean-square differences (RMSD), the determination coefficient, R_2, and the equation of the regression line complete the statistical indicators used to illustrate the results.

B. Downwelling Irradiance Estimation

It was underlined in the LISCO paper that the atmospheric transmittance normalization step leads to an increase in the data dispersion by 6% on spectral average. In Zibordi's comment, this dispersion is attributed to probable contamination by stray light perturbation or issues with the noncosine response of the HyperSAS irradiance sensor. In order to assess the quality of the HyperSAS irradiance sensor, the downwelling irradiances measured by HyperSAS, denoted by E_d (HyperSAS), were compared with the SeaPRISM irradiance estimate computed by the AERONET-OC processor as follows:

$$E_d(\mathrm{SeaPRISM}) = E_0 D^2 T_0 \cos\theta_0, \tag{3}$$

with E_0 being the extraterrestrial solar irradiance [7], D^2 accounting for variation in sun-earth distance over the year, T_0 being the atmospheric diffuse transmittance, and θ_0 the solar zenith angle. Results of the intercomparison are shown in Fig. 1. This intercomparison exhibits strong correlation between the two data sets with $R^2 > 0.97$. The |URPD| and RMSD values indicates reasonable dispersion with |URPD| = 5% and RMSD = 6.5 $\mathrm{mW\,cm^{-2}\,\mu m^{-1}}$, which is comparable to |URPD| = 4% and RMSD = 6 $\mathrm{mW\,cm^{-2}\,\mu m^{-1}}$ shown in the Zibordi comment results based on the same approach. However, the URPD value of −4.9% departs significantly from Zibordi's value of −1%. Generally the value of −4.9% is beyond cosine error range (±3%) from the specifications of the HyperSAS irradiance sensor and ∼ − 3% estimated

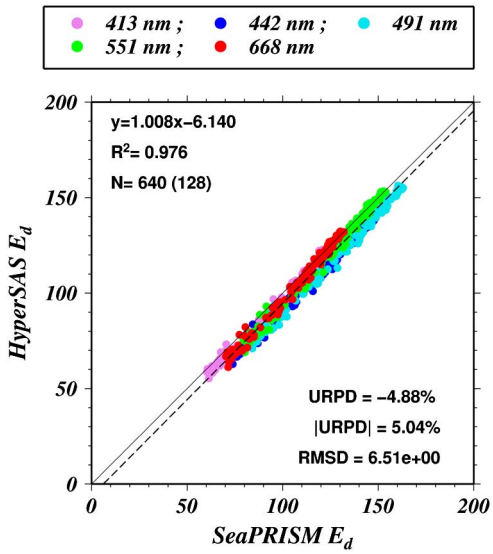

Fig. 1. (Color online) Intercomparison of the downwelling irradiance (in $\mathrm{mW\,cm^{-2}\,\mu m^{-1}}$) derived from SeaPRISM and HyperSAS measurements utilized in the intercomparison of the LISCO article.

by Zibordi [8] especially if combined with stray light impact (+1% in the 550 to 800 nm range and with up to +4% at 400 nm [9]).

Additional calibration of the irradiance sensor for noncosine response was conducted at Satlantic, Inc. to determine possible deviations of the sensor characteristics from original specifications. First, the general recalibration by Satlantic, Inc. of the HyperSAS system showed a radiometric stability, over a time period of approximately 15 months, better than 1% for the irradiance sensor. Second, the noncosine response of the sensor used for the LISCO intercomparison was precisely quantified for the full range of wavelengths and incidence angles. Based on this specification of the sensor, the resulting error on the downwelling irradiance was simulated by radiative transfer computations through the Ordres Successifs Océan-Atmosphère (OSOA) code [10]. Let us define the relative error in downwelling irradiance measurements due to nonperfect cosine response of the sensor as:

$$\Delta E_d = 100\frac{E_d^{\mathrm{mes}} - E_d^{\mathrm{true}}}{E_d^{\mathrm{true}}} \tag{4}$$

where E_d^{true} and E_d^{mes} are the downwelling irradiance computed by integration of downwelling sun and atmospheric radiances over the upper hemisphere in considering the perfect and the nonperfect cosine responses, respectively. Figure 2(a) shows the values of ΔE_d with respect to the solar zenith angle θ_s at 442, 551, and 668 nm for a purely molecular atmosphere and an aerosol optical thickness of 0.1 at 550 nm. In the green and red bands (i.e., 551 and 668 nm) the error is smaller than 1% up to solar angles of 40° and remains smaller than 4% even for solar angle as high as 60°. At 442 nm, where atmosphere is highly scattering and the amount of diffuse light is enhanced, the error due to the cosine response is more pronounced with $\Delta E_d < 2\%$ for $\theta_s < 40°$ and $\Delta E_d < 5\%$ for $\theta_s < 60°$. On the other hand, the solar angles leading to the LISCO intercomparison range from 20° to 60° as seen in the histogram of Fig. 2(b) for a distribution centered on 40°. Consequently, it can be safely concluded that the mean ΔE_d should be no larger than 2% over the period of the LISCO time series even in the blue part of the spectrum. Thus, it can be recognized that the cosine error leads to underestimation of the downwelling irradiance at LISCO site, but this negative bias cannot entirely explain the overall discrepancies observed in Fig. 1.

The observed negative bias could be also partially due to absorption behavior of the aerosols present, which typically takes place in the blue part of the visible spectrum [11,12] because low single scattering albedos (i.e., lower than 0.95) are frequently retrieved from the AERONET measurements of LISCO; see Fig. 3. Estimation of irradiance decrease due to aerosol absorption is 1% up to 2% in the red part of the spectrum and can be noticeably greater at

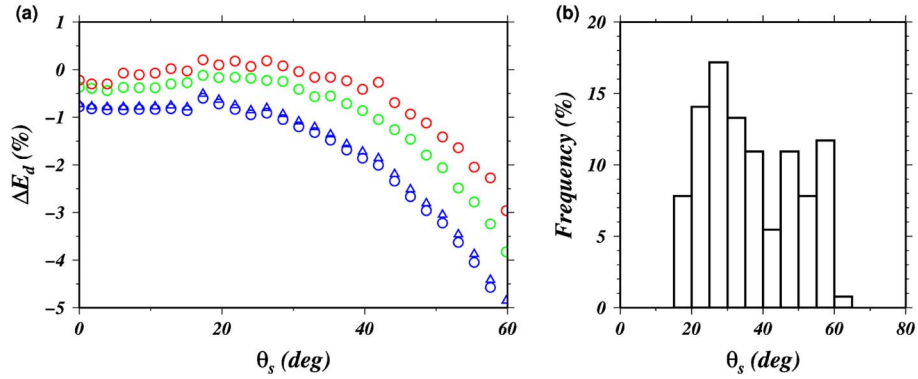

Fig. 2. (Color online) (a) Relative error in downwelling irradiance measurements due to nonperfect cosine response of the sensor for an aerosol optical thickness of 0.1 at 550 nm for the bands centered on 442 (blue circles, bottom), 551 (green circles, center), and 668 nm (red circles, top). The blue triangles hold for a purely molecular atmosphere at 442 nm. (b) Histogram of the solar zenith angles θ_s leading to the matchup comparison of Fig. 1.

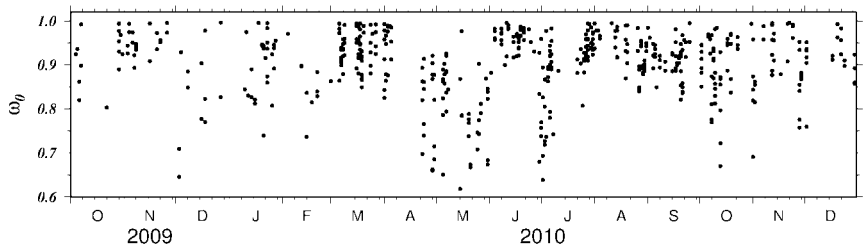

Fig. 3. Time series of the aerosol single scattering albedo ω_0 at 442 nm as retrieved by the AERONET system of the LISCO site over the period of the LISCO intercomparison analysis.

the shorter wavelengths with differences ranging from 2% to about 5% when the sun goes from zenith position to an angle of 60°, as can been seen in Fig. 4. However, only a more dedicated analysis on the correlation between the presence of absorbing aerosols and the lower downwelling irradiance measured by HyperSAS with respect to the SeaPRISM would be able to quantify the impact on the intercomparison of Fig. 1. It should also be noted that, in addition to periodic visits and control on site, the irradiance sensor, as well as the sky radiance sensor, was covered by the plate of the bio-shutter (Satlantic), which opened only for 2 min of measurements and prevented sensors from contamination by water and dust as well as from thermal degradation because of direct sun illumination, which led to minimal changes in calibration over the 2 year period.

C. Water-Leaving Radiance Derivation

One of the major advantages of the LISCO instrumentation set is that HyperSAS and SeaPRISM instruments acquire data almost concurrently, but with different viewing geometries as the day progresses, except for the time when the sun is exactly south when both instruments point west. However, it should be pointed out that directional fluctuations in the measured sea radiance are also induced by the sun and sky light reflections on the ruffled surface, which in the end may create significant uncertainties in the retrieved water-leaving radiance. Thus, relatively higher discrepancies between the two systems in determination of water-leaving radiance compared to the results presented in the comment letter [6] can be partially attributed to the fact that sea radiance measurements of SeaPRISM and HyperSAS have been acquired at different relative azimuth angles, as pointed out in [6]. This results in very different contributions of reflected sky radiances and the necessity of the bidirectional reflectance distribution function (BRDF) correction of water-leaving radiances [13]. Nevertheless, the data processing was originally designed for different azimuth configurations, and application of this processing on HyperSAS is expected to yield virtually similar normalized water-leaving radiances for measurements performed within the limited azimuth range used in Harmel *et al.* [5].

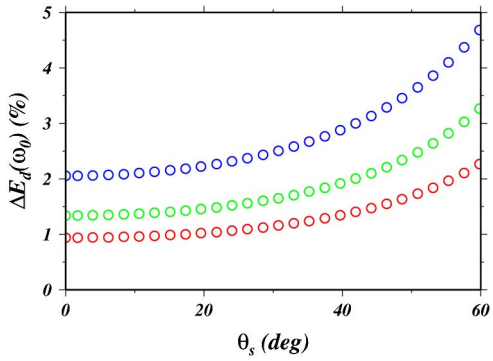

Fig. 4. (Color online) Relative difference between the downwelling irradiances calculated for nonabsorbing aerosol ($\omega_0 = 1$) and for absorbing aerosol ($\omega_0 = 0.9$). Simulations have been carried out with the radiative transfer code OSOA for an aerosol optical thickness of 0.1 at 550 nm and for the bands centered on 442 (blue circles, top), 551 (green circles, center), and 668 nm (red circles, bottom).

It should also be noted that the water-leaving radiances retrieved at the LISCO site are lower (around 0.3 and 0.8 mW cm^{-2} sr^{-1} μm^{-1} for the spectral average and at 551 nm, respectively; see Table 1) than those retrieved at the Acqua Alta Oceanographic Tower and discussed in Zibordi's comment (around 1.2 mW cm^{-2} sr^{-1} μm^{-1} on average). This partly explains the higher URPD values observed for the LISCO data because of lower values in the denominator of Eq. (1) because the RMSD value computed for intercomparison of the water-leaving radiances normalized by the HyperSAS downwelling irradiance remains low, namely 0.068 mW cm^{-2} sr^{-1} μm^{-1}, and comparable to the results of Zibordi's comment exhibiting RMSD around 0.08 mW cm^{-2} sr^{-1} μm^{-1} for intercomparisons of normalized water-leaving

Table 1. Average and Standard Deviation of L_{WN} at 551 nm and for all the Wavelengths between 413 and 668 nm, Solar Zenith Angle, Aerosol Optical Thickness τ_a at 551 nm, and Wind Speed for the Measurement Conditions Leading to the Construction of SeaPRISM and HyperSAS Matchup Intercomparisons

Quantity	Average ± Standard Deviation
L_{WN} (551 nm) (mW cm^{-2} sr^{-1} μm^{-1})	0.80 ± 0.24
L_{WN} all wavelengths (mW cm^{-2} sr^{-1} μm^{-1})	0.35 ± 0.30
Solar zenith angle (deg)	39.9 ± 13.6
τ_a(555 nm)(–)	0.09 ± 0.04
Wind speed (ms^{-1})	6.6 ± 2.1

radiances retrieved from in-water and SeaPRISM systems.

On the other hand, these discrepancies are observed to be significantly smaller for the restricted range of azimuth angles when both instruments are pointed approximately in the same direction. But further analysis also showed that some discrepancies are due to the different response of the HyperSAS and SeaPRISM to the same filtering procedures because of the longer integration time of HyperSAS (2 s) in comparison with SeaPRISM (75 ms) as pointed out in the comment letter [6]. Specifically, the procedure that was attributed in [5] for the removal of the residual sun glint following terminology described in [4] utilizes the average of the lowest 5% sea radiance measurements, denoted as L_T^*, for further processing instead of the average of all L_T values. It should be noted that the use of this procedure was thereafter reattributed to the minimization of perturbing effects of sea surface roughness in L_T [1]. When applied to HyperSAS processing, it is observed that the procedure primarily eliminates the remaining sun glint component that was not eliminated by other filtering procedures established in [5] for HyperSAS.

At this point, comparisons between the L_T^* of HyperSAS, which is obtained by averaging the lowest 5% of L_T values, and quality-assured SeaPRISM level 1.5 average L_T values (i.e., skipping the excessive sky-glint contributions removal step) are further carried out. Here, both L_T^* of HyperSAS and average L_T of SeaPRISM data can be considered free of sun-glint perturbation effects as the sun-glint-infected measurements have been effectively filtered out by taking the lowest values in the case of HyperSAS [5] and by using a favorable measurement geometry and by accounting for field constraints [1] in the case of SeaPRISM as well as by applying the respective data quality process of both systems. These com parisons exhibit significantly smaller discrepancy between the two systems even for a broad range of azimuth angles (i.e., $70° \le \varphi \le 180°$), as can be readily seen in Fig. 5. The spectral average discrepancy value (URPD) between the sea radiance data of HyperSAS and SeaPRISM decreased to 3% from 8.15% before for the comparisons carried out using L_T^* data of both instruments.

For the restricted azimuth angle range (i.e., $80° \le \varphi \le 100°$), which permits minimization of the impact of both the bidirectionality dependence and the differences in the surface-reflected radiance contributions to the water-leaving radiance derivations from HyperSAS and SeaPRISM datasets, the difference between two datasets is becoming almost insignificant as shown in Fig. 5(b). Using the same data presented in the above figure, the sky-reflection removal step is further processed to obtain water-leaving radiance, L_w, data. The comparisons between the resulting L_w of SeaPRISM and HyperSAS are shown in Fig. 6. In this case, the removal of the sky radiance L_s to arrive at water-leaving radiances L_w leads to the small increase in URPD to 9% in comparison with 3.16% for total sea radiance comparison for the broad range of azimuth angles, mostly due to low values of water-leaving radiance in the blue part of the spectrum and the remaining necessity of BRDF correction [Fig. 6(a)]. However, for the restricted range of azimuth angle range, discrepancy between the two data sets is very low with URPD value equal to 0.38%, and bias is also found to be negligible [Fig. 6(b)]. For normalized water-leaving radiance, L_{WN}, these comparisons should depend only on the differences in E_d, which were discussed above.

On the other hand, the transformation from L_T to L_T^* for the SeaPRISM eliminates the additional component from the SeaPRISM data that has sky spectral shape for most of the measurements but close to sun-glint spectrum in the morning. This transformation accounts for about 7% increase in URPD value even for the restricted azimuth angle range. Obviously SeaPRISM data is very sensitive to this correction and, as pointed out in [1] and the comment

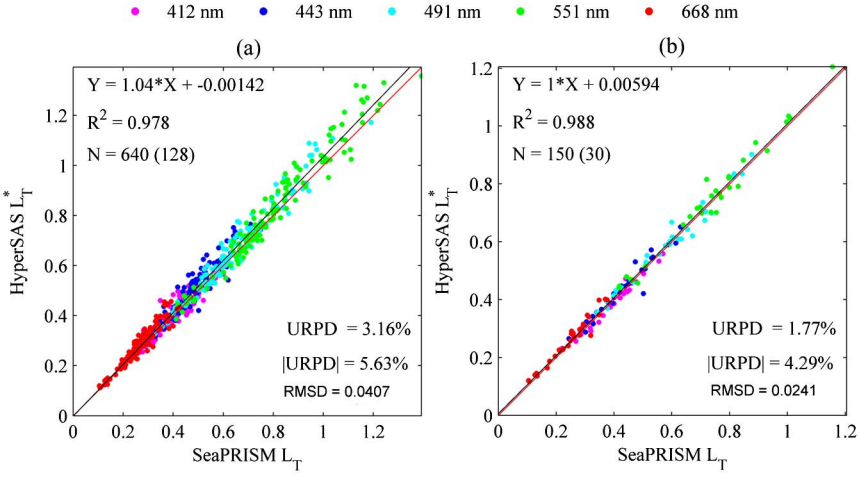

Fig. 5. (Color online) Intercomparison of the total sea radiance (in $\mathrm{mW\,cm^{-2}\,sr^{-1}\,\mu m^{-1}}$) of SeaPRISM ($L_T$) and HYPERSAS ($L_T^*$). (a) $70° \le \varphi \le 180°$ range, (b) $80° \le \varphi \le 100°$ range.

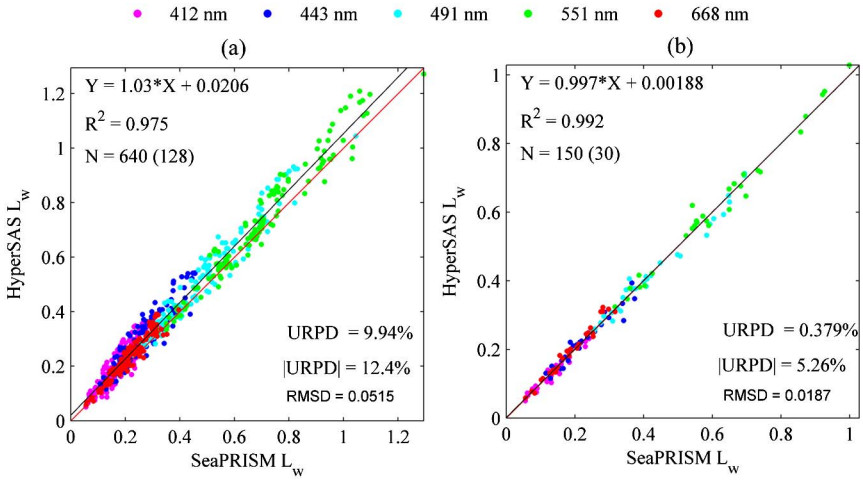

Fig. 6. (Color online) Intercomparison of the nonnormalized water-leaving radiance, L_w, (in $\mathrm{mW\,cm^{-2}\,sr^{-1}\,\mu m^{-1}}$) of SeaPRISM and HYPERSAS. (a) $70° \le \varphi \le 180°$ range, (b) $80° \le \varphi \le 100°$ range.

paper by Zibordi [6], can lead to an overcorrection of sky-glint perturbations. At the same time, it can also be argued that this possible sky-glint perturbation effect might not be properly removed from HyperSAS data in the L_T to L_T^* transformation procedure due to the HyperSAS instrument's relatively longer integration time. Because sky perturbations are more common than sun-glint effects, it is possible that during 2 s of HyperSAS integration time these sky components are averaged and exist in HyperSAS L_T^* as an additional background. In the current version of the above-water data processing this L_T to L_T^* transformation procedure is therefore a significant source of uncertainty whether for short (SeaPRISM) or long (HyperSAS) integration time.

3. Commentary

The two LISCO data sets were reconciled when the first step of the above-water standard algorithm, L_T to L_T^* transformation, is discarded in the SeaPRISM data processing, leading to URPD value close to 1%. This indicates that this step is critical when dealing with low water-leaving radiances, which is especially the case for the LISCO waters at the shorter wavelengths. Moreover, the sky glint is more pronounced in this part of the spectrum due to the high Rayleigh scattering of the atmosphere. It should be noted that the reflection factor of the ruffled sea surface used in AERONET-OC and HyperSAS processing were calculated based on radiative transfer computation and the Cox and Munk model to handle the wave slopes' distribution [14,15]. That means that all the radiances from any direction of the sky were integrated to derive the sky-glint component via the sea reflection factor computation. However, such a use of the Cox and Munk model can produce errors of about 40% in the calculated radiance when applied to a small portion of the sea surface, such as surfaces of a couple of square meters, in comparison to a more realistic model of the wave slopes distribution [16]. Along these lines, analysis of the performance of the sea surface correction procedure based on refined statistical models of wave statistics is one of the main perspectives of this work.

The preliminary filtering of the data (L_T to L_T^* transformation), which are affected by residual sun glint and specular reflection of extremely bright portions of the sky, might add bias to the approximations done for the sky-glint computation based on complete radiative transfer simulations. For instance, the sky glint can be diminished by capillary waves reflecting darker portions of the sky or by the shadow of the waves themselves [17]. Thus, the systematic use of the minimum value of the sea radiance measurement sequence followed by the proper sky-glint correction based on radiative transfer computation might overestimate the sky-glint contribution when short time integration and small field of view are combined, as is the case of the SeaPRISM system and as stated in [1]. At the same time, it can also be argued that this possible excessive sky-glint perturbation or residual sun-glint contribution might not be properly removed from HyperSAS data in the L_T to L_T^* transformation procedure due to the HyperSAS instrument's relatively longer integration time. In conclusion, further analysis of the correction for surface-reflected light are recommended and should be achieved based on full radiative transfer computations, including accurate modeling of the capillary waves dynamic [16,18–20], which play an important role on light reflection when dealing with small field of view and short time integration [21].

We would like to thank G. Zibordi for the attention to the issues that led to the clarification of the filtering procedures and effects in above-water radiometric measurements and estimations of downwelling irradiance. We would also like to thank Satlantic, Inc., a leading manufacturer of the sensors for the ocean color community, for an expedited recalibration of our irradiance sensor for cosine effects and taking immediate steps for minimization of noncosine responses.

References

1. G. Zibordi, B. N. Holben, I. Slutsker, D. Giles, D. D'Alimonte, F. Mélin, J. F. Berthon, D. Vandemark, H. Feng, and G. Schuster, "AERONET-OC: a network for the validation of ocean color primary radiometric products," J. Atmos. Ocean. Technol. **26**, 1634–1651 (2009).
2. F. Mélin, G. Zibordi, and J. F. Berthon, "Assessment of satellite ocean color products at a coastal site," Remote Sens. Environ. **110**, 192–215 (2007).
3. S. W. Bailey and P. J. Werdell, "A multi-sensor approach for the on-orbit validation of ocean color satellite data products," Remote Sens. Environ. **102**, 12–23 (2006).
4. S. B. Hooker, G. Lazin, G. Zibordi, and S. McLean, "An evaluation of above- and in-water methods for determining water-leaving radiances," J. Atmos. Ocean. Technol. **19**, 486–515 (2002).
5. T. Harmel, A. Gilerson, S. Hlaing, A. Tonizzo, T. Legbandt, A. Weidemann, R. Arnone, and S. Ahmed, "Long Island Sound Coastal Observatory: assessment of above-water radiometric measurement uncertainties using collocated multi and hyperspectral systems," Appl. Opt. **50**, 5842–5860 (2011).
6. G. Zibordi, B. N. Holben, I. Slutsker, D. Giles, D. D'Alimonte, F. Mélin, J. F. Berthon, D. Vandemark, H. Feng, G. Schuster, B. Fabbri, S. Kaitala, and J. Seppala, "Long Island Sound Coastal Observatory: assessment of above-water radiometric measurement uncertainties using collocated multi and hyperspectral systems: comment," Appl. Opt. **51**, 3888–3892 (2012).
7. G. Thuillier, M. Herse, D. Labs, T. Foujols, W. Peetermans, D. Gillotay, P. C. Simon, and H. Mandel, "The solar spectral irradiance from 200 to 2400 nm as measured by the SOLSPEC spectrometer from the ATLAS and EURECA missions," Sol. Phys. **214**, 1–22 (2003).
8. G. Zibordi and B. Bulgarelli, "Effects of cosine error in irradiance measurements from field ocean color radiometers," Appl. Opt. **46**, 5529–5538 (2007).
9. S. McLean, Radiometric Data Processing Course, Ocaen Optics XIX Conference, Barga, Italy.
10. M. Chami, R. Santer, and E. Dilligeard, "Radiative transfer model for the computation of radiance and polarization in an ocean-atmosphere system: polarization properties of suspended matter for remote sensing," Appl. Opt. **40**, 2398–2416 (2001).
11. Gordon, Du, and Zhang, "Remote sensing of ocean color and aerosol properties: resolving the issue of aerosol absorption," Appl. Opt. **36**, 8670–8684 (1997).
12. C. Moulin, H. R. Gordon, R. M. Chomko, V. F. Banzon, and R. H. Evans, "Atmospheric correction of ocean color imagery through thick layers of Saharan dust," Geophys. Res. Lett. **28**, 5–8 (2001).
13. S. Hlaing, A. Gilerson, T. Harmel, A. Tonizzo, A. Weidemann, R. Arnone, and S. Ahmed, "Assessment of a bidirectional reflectance distribution correction of above-water and satellite water-leaving radiance in coastal waters," Appl. Opt. **51**, 220–237 (2012).
14. C. D. Mobley, "Estimation of the remote-sensing reflectance from above-surface measurements," Appl. Opt. **38**, 7442–7455 (1999).
15. C. Cox and W. Munk, "Measurement of the roughness of the sea surface from photographs of the sun's glitter," J. Opt. Soc. Am. **44**, 838–850 (1954).
16. S. Kay, J. Hedley, S. Lavender, and A. Nimmo-Smith, "Light transfer at the ocean surface modeled using high resolution sea surface realizations," Opt. Express **19**, 6493–6504 (2011).
17. M. Sancer, "Shadow-corrected electromagnetic scattering from a randomly rough surface," IEEE Trans. Antennas Propag. **17**, 577–585 (1969).
18. Y. You, D. Stramski, M. Darecki, and G. W. Kattawar, "Modeling of wave-induced irradiance fluctuations at near-surface depths in the ocean: a comparison with measurements," Appl. Opt. **49**, 1041–1053 (2010).
19. Y. You, G. W. Kattawar, K. J. Voss, P. Bhandari, J. Wei, M. Lewis, C. J. Zappa, and H. Schultz, "Polarized light field under dynamic ocean surfaces: numerical modeling compared with measurements," J. Geophys. Res. **116**, C00H05 (2011).
20. M. Ottaviani, R. Spurr, K. Stamnes, W. Li, W. Su, and W. Wiscombe, "Improving the description of sunglint for accurate prediction of remotely sensed radiances," J. Quant. Spectrosc. Radiat. Transfer **109**, 2364–2375 (2008).
21. S. Kay, J. D. Hedley, and S. Lavender, "Sun glint correction of high and low spatial resolution images of aquatic scenes: a review of methods for visible and near-infrared wavelengths," Remote Sens. **1**, 697–730 (2009).